Fracture Mechanics of Concrete Structures
Proceedings FRAMCOS-3
AEDIFICATIO Publishers, D-79104 Freiburg, Germany

NUMERICAL STUDIES ON THE DOUBLE-EDGE NOTCHED MODE II GEOMETRY

J. Ozbolt, H.W. Reinhardt, and S. Xu,
Institute of Construction Materials, University of Stuttgart, Stuttgart, Germany

Abstract

The analysis of concrete members under shear action requires reliable material parameters. A new testing method (double-edge notched compression test) has been developed which yields pure mode II. Recently, tests have been performed on a high strength concrete (cylinder compressive strength of 85 MPa) which confirm the theoretical predictions. In the present paper the new testing method is numerically investigated and the results are compared with experimental and analytical solutions.

Key words: Numerical study, mode II tests, double-edge notched specimens, high strength concrete.

1 Introduction

When a structural engineer analyses a structural member it is quite common to distinguish between normal forces, bending moments and shear forces and to reinforce concrete accordingly. As bending shear is concerned, a part of the shear force is taken by the concrete compression zone, another by the stirrups, a third by the dowel action of the longitudinal reinforcement and a forth by the aggregate interlock in the crack. All sections of a structure are checked and reinforced according to the shear action. In such an approach, equilibrium of outer and inner forces has to be reached and compatibility of displacements has to be satisfied.

Looking closer to shear there are three stages involved: first, as long as the concrete is uncracked there are two principal normal stresses (plane stress condition); second, a crack forms perpendicular to the principal tensile stress direction; third, a sliding motion introduces shear along the crack faces. In terms of fracture mechanics, there is always a strong K_I and a weak K_{II} in the beginning. With crack extension and redistribution of stresses, however, mode II becomes more important on a lower stress level. There are exceptions where mode II prevails right from the beginning. These are joints between dissimilar media under shear forces and normal forces parallel to existing cracks. For these cases a pure mode II testing should be available.

2 Mode II fracture - theory and experiments

In the past a number of testing methods for mode II fracture have been proposed and applied to various materials (Reinhardt et al., 1997). Although there are several methods proposed for mode II testing there is none of them which produces a pure mode II situation. Either by eccentric loading or by deformation during testing a mode I contribution cannot be avoided which makes these testing arrangements mixed mode devices. Recently a new testing method for wood and concrete based on the double-edge notched plate specimen has been proposed.

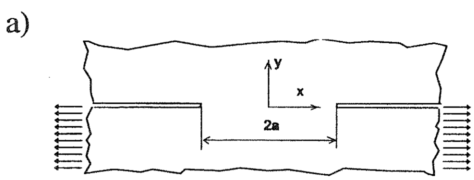

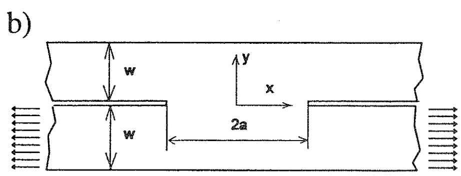

Fig. 1. Double-edge notched specimen: a) infinite plate, b) infinite strip

Fig. 1a shows the geometry of a double-edge notched infinite plate under in-plane tensile loading. The ligament length is $2a$. Tada's (Tada et al., 1985) elastic solution yields:

$$K_{II} = \frac{\sigma}{4}(\pi a)^{1/2} \tag{1}$$

It is important to notice that K_I vanishes and K_{II} remains as the only stress component. This theoretical solution is valid for an infinite plate and the question is whether it is also applicable to a specimen of finite size.

The finite plate (see Fig. 1b) can be analyzed using the J-integral method (Rice, 1986; Radaj and Zhang, 1991). The solution yields (Xu et al., 1997):

$$K_{II} = \frac{\sigma}{4}(w)^{1/2} \tag{2}$$

The same result has been obtained by various authors (Keer, 1974; Yahsi and Gcmen, 1987) who used other mathematical tools when they analyzed the contact problem of two perfectly bonded infinite strips of dissimilar materials. The special case of the two equal materials and same width leads to Eq. (2) and $K_I = 0$. From Kerr (1974) it is concluded that a finite length of the strip $h \geq 2a$ can be assumed to be infinite. Using this knowledge, a new specimen geometry for pure shear testing was designed (Reinhardt et al., 1997). The new method is called double-edge notched compression test (DENCT). The length of the specimen h should be $\geq 2a$ in order to apply (2). Furthermore, for $h \geq 2a$ and $w \geq \pi a$ (1) applies.

In order to measure K_{II}, experiments on double-edge notched concrete test specimens have been carried out (Reinhardt et al., 1997). To support and to confirm the experimental and analytical results for DENCT test specimen the above mentioned experiments are numerically simulated. In the following paragraphs, the results of the numerical study are presented and compared with the experimental data.

3 Numerical study

Numerical studies were performed for the same concrete and the same specimen geometry as in the experiments (Reinhardt et al., 1997). The dimensions of the specimens were 150 x 150 x 100 mm^3 (see Fig. 2). The width of the notch was constant and equal to 4 mm. The concrete properties used in the analysis were: f_c = 85 MPa, f_t = 5 MPa, G_F = 80 N/m, d_a = 16 mm and Young's modulus E = 30000 MPa. In contrast to the experiments, where the ligament length was varied only from a = 35 to 45 mm, in the analysis the ligament length was varied as a = 15, 30, 45 and 60 mm. The compressive load was applied by control of vertical displacement on the load-surfaces (see Fig. 2). The loading surface in direction perpendicular to the load was assumed to be unconstrained.

The analysis was carried out using a nonlocal plane strain FE code based on the microplane material model for concrete (program *MASA*) (Ozbolt et al., 1997; Ozbolt and Bazant, 1996).

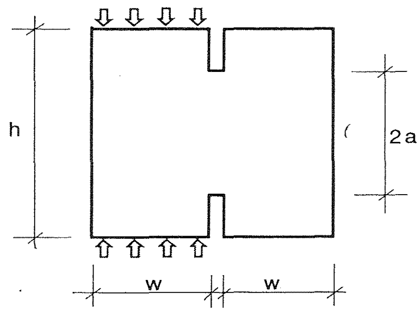

Fig. 2. Geometry and load of DENCT specimen

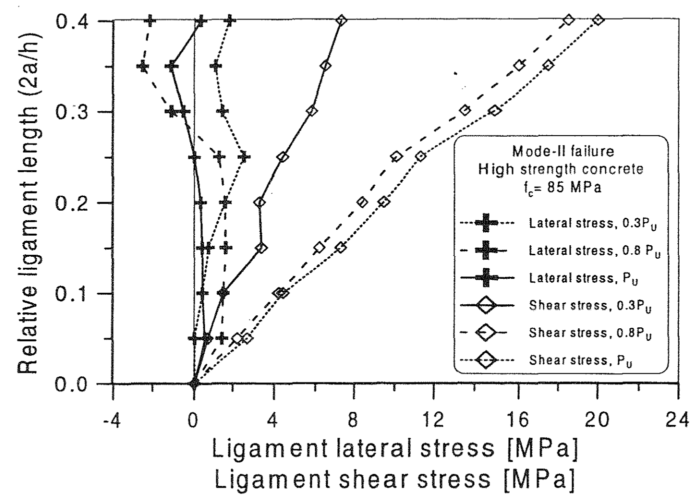

Fig. 3. Distribution of lateral and shear stresses over the mid of the ligament length for a = 30 mm and 30%, 80% and 100% of ultimate load

To demonstrate that the double-edge notched geometry generates a pure mode-II failure, Fig. 3 shows the distribution of nodal lateral (σ_{xx}) and shear (σ_{xy}) stresses plotted over half of the ligament length (vertical cross-section) for a specimen with a = 30 mm. The stresses are shown at 30%, 80% and 100% of the ultimate load. Independent of the load level the lateral stresses over the vertical mid plane ligament section are close to zero. Actually, zero values lie not exactly on the vertical mid-plane but somewhere inside the notch width i.e. zero lateral stress plane is not exactly vertical (plane). The exact position of zero lateral stresses over the ligament length at 80% of ultimate load is plotted in Fig. 4. The figure shows the distribution of the lateral stresses over the horizontal planes at different positions of the ligament. It proves that for double-edge notched test specimen, there is a pure mode-II failure condition.

In Figs. 5a and b the principal strain patterns are plotted for the specimen with $a = 30$ mm. The figures show the mode II crack at peak load and in the post peak regime (approximately 50% of the ultimate load), respectively. At the notch front the crack is inclined at an angle of approximately 30^0 and in the mid of the specimen it is vertical. This agrees with the shape of the neutral line discussed above (see Fig. 4). In spite of the concrete compression failure, in the compressed part of the specimen, mode II crack develops up to it's full length. It separates the damaged (compressed) and undamaged part of the specimen, similar as in the experiments (Reinhardt, et al., 1997). Figs. 5a and b show typical diagonal compression failure of concrete short after the peak load and at about 20% of the peak load, respectively.

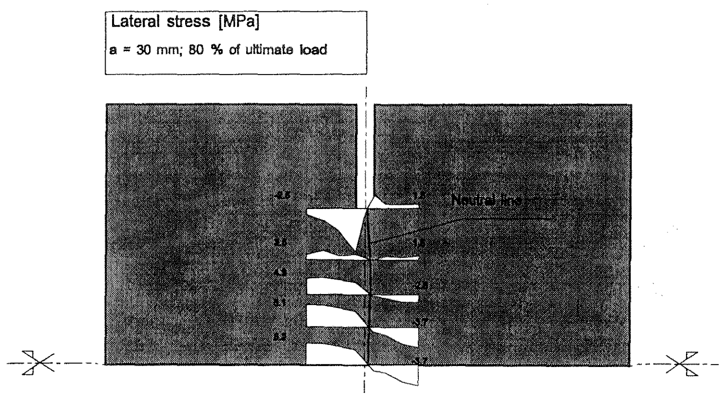

Fig. 4. Distribution of lateral stresses over the ligamant length

Similar to the experimental results, the numerical analysis shows that the specimens fail always in compression. Calculated ultimate stresses (see Table 1) decrease when the ligament length increases. Before compressive failure occurs, mode-II crack initiates. Closely after it's initiation mode-II crack growth is arrested and, instead, more critical diagonal shear failure in compression is initiated. However, in the post-peak regime mode II crack starts to grow again (compare Fig. 5c and d). In Fig. 6a is the calculated load-displacement curve plotted for a specimen with $a = 45$ mm. For comparison, in the same figure the experimentally measured curve is also plotted. As may be seen, the agreement between numerical and experimental results is good.

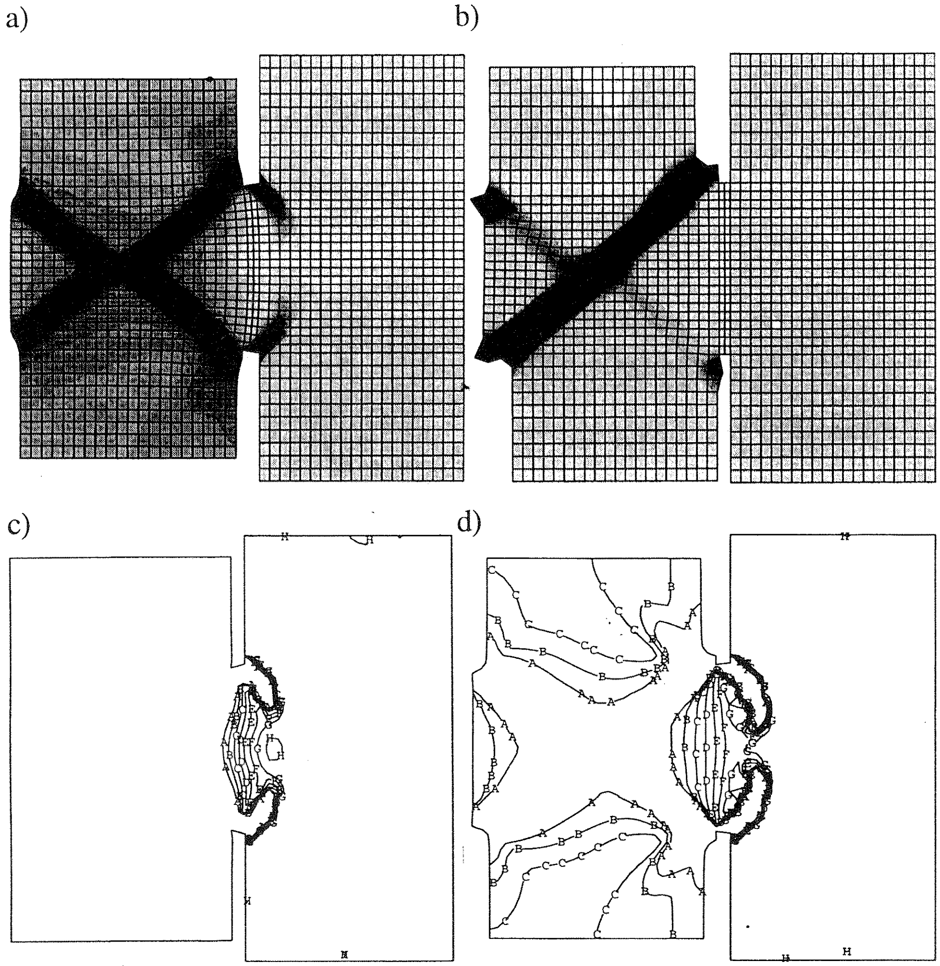

Fig. 5. Principal strain fields for specimen with a =30 mm : a) post-peak (95% of the peak load), b) post-peak (20% of the peak load), c) peak load iso-strains, max. strain = 0.002 and d) post-peak (50% of the peak load), max. strain = 0.002

To estimate the compressive stress at which mode-II cracks initiate, the distribution of shear stresses at the notch tip is plotted as a function of the compressive stress for each geometry. For illustration, Fig. 6b shows this plot for specimen with $a = 30$ mm. As one can see, for compressive stress of approximately $0.75 f_c$ the shear stress at the notch tip reaches the maximum (critical) value i.e. by further loading the shear stress remains approximately constant. Performing the above procedure for each ligament length we obtain critical shear stresses and corresponding critical compressive stresses. These values are summarized in Table 1.

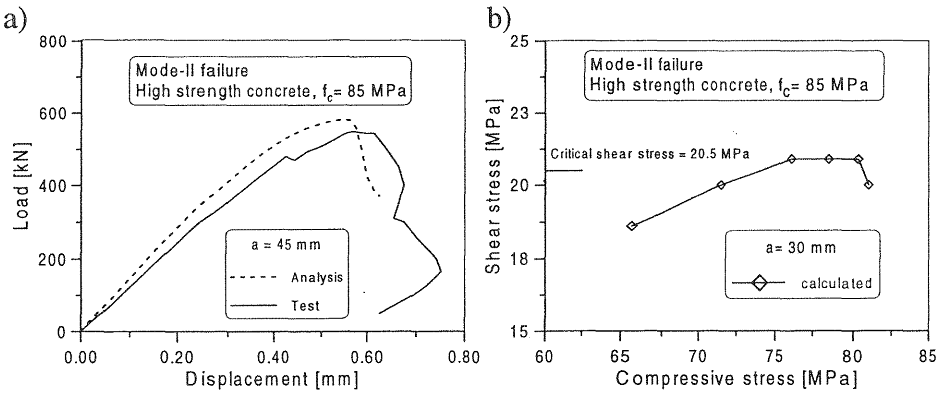

Fig. 6 a). Load-displacement curves obtained in numerical analysis and measured in experiments for $a = 45$ mm; b) Shear stresses at the notch front as a function of the compressive stress obtained from the numerical study for $a = 30$ mm

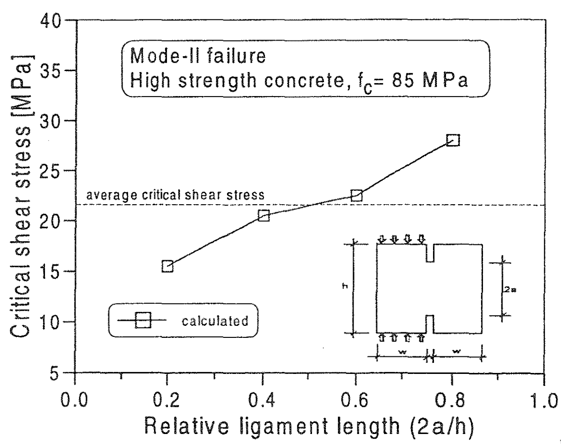

Fig. 7. Critical shear stress as a function of the relative ligament length -- numerical results

In Fig. 7 the critical shear stresses are plotted as a function of the relative ligament length. As may be seen for $0.3h < a < 0.7h$ the critical shear stress is approximately constant and in average $\tau_c = 21.5$ MPa. For $a/h < 0.3$ the critical shear stress tends to zero i.e. if the ligament length is too short (less than approximately max. aggregate size), mode-II failure cannot be realized since the stress-strain distribution is close to be uniform (uniaxial compression). On the contrary, if the ligament length is larger than $0.7h$, the critical shear strength tends to increase. The reason is due to the fact that the notch tip is too close to the concrete loading surface and therefore the influence of the boundaries is too strong.

Table 1. Mode-II failure, numerical results, f_c = 85 Mpa; [1] according to Eq. (1); [2] according to Eq. (2)

$a\,[mm]$	$\sigma_u\,[MPa]$	$\tau_c\,[MPa]$	$\sigma_c\,[MPa]$	$K_{II}\,[MPa\sqrt{m}]$
15	82.2	15.5	81.5	4.42[1]
30	81.0	20.5	68.6	4.63[2]
45	77.5	22.5	61.8	4.17[2]
60	76.2	28.0	63.9	4.32[2]

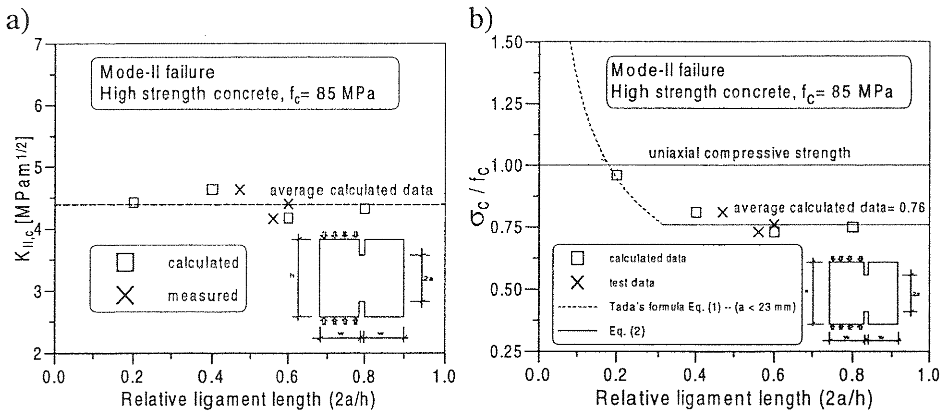

Fig. 8 a). Critical K_{II} obtained using (1) or (2), respectively, - numerical and experimental results, b) Critical compressive stress as function of the relative ligament length - numerical and test results compared with (1) and (2), respectively, under the assumption that for $a > w/\pi$, $\sigma_c = 0.76 f_c$

Based on the results shown in Table 1, from known critical compressive stresses $K_{II,c}$ values are calculated using Tada's formula for $a < w/\pi$ and Eq. (2) for $a > w/\pi$ (see Table 1) and plotted in Fig. 8a as a function of the relative ligament length. As may be seen, although the critical shear stress is not constant $K_{II,c}$ as well as σ_c for $a > w/\pi$ are approximately constant i.e. independent on the ligament length. The average calculated value obtained in the numerical analysis is 4.39 MPa$\sqrt{m}$. For comparison, in the same figure the test results are also shown. As one can see, the agreement is good. Fig. 8a confirms that for the present geometry Tada's formula and Eq. (2) give a good estimation of $K_{II,c}$. Namely, $K_{II,c}$ values were calculated based on the critical compressive stresses which correspond to the critical shear stresses obtained from the numerical study.

In Fig. 8b the relative critical compression stresses are plotted as a function of the relative ligament length. Calculated and test data are compared with the predictions of Tada's formula (1) and (2), assuming that for $a = w/\pi$ σ_c = average calculated value from the numerical study ($\sigma_c = 0.76 f_c = 64.6$ MPa). Fig. 8b shows that for $a > w/\pi$ the critical compressive stress is approximately constant i.e. independent of the ligament length. This is in good agreement with theoretical prediction (see Eq. 2). However, for $a < w/\pi$ the critical compressive stress increases what is again in good agreement with theoretical prediction based on Tada's formula. For $a \le h/10$ the critical compressive stress approximately coincides with the uniaxial compressive strength.

Numerical results, test results as well as theoretical predictions are in good agreement. The study indicates that for $a > w/\pi$ the critical compressive stress is reached at approximately $\sigma_c = 0.75 f_c$ and for this concrete $K_{II,c} = f_c/19$ with $K_{II,c}$ in MPa$\sqrt{m}$ and f_c in MPa. Whether this relation is true for other concrete strengths has to be confirmed by further experimental numerical studies.

4 Discussion of the results

According to our knowledge, at present there is no test method which is able to generate a pure mode-II failure. Most test setups generate so-called mixed mode failures. The numerical results show that the double-edge notched specimen exhibit pure mode-II conditions during the entire load history. The results show that after mode-II crack initiation its further propagation is arrested and overriden by more critical diagonal shear failure in compression. Consequently, mode-II fracture energy, similar as in the experiment, could not be measured from calculated load-displacement curves.

The calculated data exhibit good agreement with the experimental results. The present study has yielded $K_{II,c}$ values which are in good agreement with values estimated from other researches (Swartz and Taha, 1990; Banks-Sills and Arcan, 1983). The average calculated value for $K_{II,c}$ was 4.38 while the average test data (Reinhardt et al., 1997) was almost the same and equal to 4.40 MPa$\sqrt{m}$. The critical stress intensity factor $K_{I,c}$ may be in the order of 1 MPa$\sqrt{m}$ which is about a fifth of $K_{II,c}$. If we assume that fracture energy G_F is proportional to the critical energy release rate G_c and since $K = \sqrt{GE}$ it would mean that $G_{II,F}$ is about 25 times as large as $G_{I,F}$.

5 Conclusions

- The numerical results confirmed that the new testing method based on the double-edge notched compression test specimen exhibits a pure Mode-II failure type.
- After initiation of the mode-II crack its further propagation is arrested by diagonal shear failure of concrete under compression. After the peak load is reached the mode II crack propagates again.
- Due to the strong influence of the compressive concrete failure it is not possible to calculate $G_{II,F}$ from the load-displacement curve, however, it is possible to calculate the critical stress intensity factor $K_{II,c}$.
- The numerical results agree well with the experimental and analytical results. They have demonstrated the validity of the new testing method for pure mode II.

6 References

Banks-Sills, L., Arcan, M. (1983) An edge-cracked mode II fracture Specimen, **Experimental Mechanics,** 23, 257- 261.

Keer, L.M. (1974) Stress Analysis for Bonded Layers, **JAM,** 41, 679-683.

Keer, L.M., Guo, Q. (1990) Stress Analysis for Symmetrically Loaded Bonded Layers, **IJF**, 43, 69-81.

Ozbolt, J. and Bazant, Z.P. (1996) Numerical smeared fracture analysis: nonlocal microcrack interaction approach, **IJNME,** 39, 631-661.

Ozbolt, J., Li, Y.-J., and Kozar, I. (1997) Microplane model for concrete, Submitted to **IJSS**.

Radaj, D., Zhang, S. (1991) Stress Intensity Factors for Spot Welds Between Plates of Unequal Thickness, **EFM,** 39, No. 2, 391-413.

Reinhardt, H.W., Ozbolt, J., S. Xu, and Dinku, A. (1997) Shear of Struc. Concrete Members and Pure Mode II Testing, **ACBM**, 5, 75-85.

Rice, J.R. (1968) A Path Independent Integral and the Approximate Analysis of Strain Concentrations by Notches and Cracks, **JAM,** 35, No. 2, 379-386.

Swartz, S.E., Taha, N.M. (1990) Mixed Mode Crack Propagation and Fracture in Concrete, **EFM**, 35, No. 1/2/3, 137-144.

Tada, H., Paris, P., Irwin, G. (1985) The Stress Analysis of Cracks Handbook (2nd edition), **Paris Productions Incorporated**, St. Louis.

Xu, S., Reinhardt, H.W., Gappoev, M. (1996) Mode II Fracture Testing Method for Highly Orthotropic Materials like Wood, **IJF,** 75, 185-214.

Yahsi, O.S., Gcmen, A.E. (1987) Contact Problem for Two Perfectly Bonded Dissimilar Infinite Strips, **IJF**, 34, 162-177.